



A complex slope deformation case—history

Abstract Slope movements represent a class of phenomena, which can display a great variety of styles, sizes and displacement rates. Some are extremely rapid, short-lived and highly destructive; others are extremely slow and apparently endless. This paper describes an extremely slow soil slope deformation process that is probably active since thousands of years and will certainly go on for many years to come. The results of in-depth investigations carried out after the 1980 Irpinia-Basilicata earthquake integrated by satellite images covering the time interval 1992–2013 have provided a global and consistent framework that allows to draw a reliable scenario about the effects of the geological processes that are active in the area on slope deformation mechanisms.

Keywords Slope deformation · Erosion · Earthquake · Displacement field · Pore pressure regime

Foreword

Landslides are widespread in the Apennines chain in Italy. Some, such as falls, slides in brittle soils, debris flows and debris avalanches are rapid, short-lived and highly destructive; others, such as slides in ductile fine-grained soils, are extremely slow. In particular, peculiar slope movements such as spreads and slope deformation phenomena (Hungur et al. 2014) are quite well represented all along the chain sometimes involving small urban centres built on the top of hills. These slow movements generally raise delicate issues concerning the land use, due to their generally complex mechanisms that do not allow any reliable prediction of future evolution. On the other hand, stabilizing these often huge soil/rock masses is practically impossible. However, as experience suggests, living in such unstable areas is sometimes possible even though based on an expensive maintenance of structures and infrastructures.

This paper describes a peculiar and complex slope deformation process that involves the hill on the top of which the old Bisaccia village rises. Monitoring of the area over about 40 years and in-depth geotechnical and numerical analyses allowed providing a comprehensive picture of the overall deformation field and a consistent interpretation of the main governing mechanical processes.

The Bisaccia hill and its geomorphological setting

Bisaccia hill (Fig. 1) is located in the Southern Apennines chain, 135 km North-East to Naples, Italy. It is a thick elongated platform extending in the South-North direction, which consists of slightly cemented polygenic Pliocene conglomerates overlying the Tertiary tectonized “Argille Varicolori” formation, a deep deposit essentially constituted by high plastic clay shales (Ogniben 1969; D’Argenio et al. 1973; Bonardi et al. 1988).

The conglomerate deposit fills a synclinal that is subjected to intense erosion phenomena, which led to formation of two narrow parallel valleys that bound the eastern and western sides of the hill (Fig. 1a), the eastern “Vallone dei Corvi” and the western “Vallone Ferrelli”. As a matter of fact, erosion has completely dismantled the conglomerates and is rapidly deepening into the fine-grained bedrock. The hill is cyclically hit by earthquakes. The last strong events occurred on July, 23, 1930 ($M = 6.7$), on August, 21, 1962 ($M = 6.4$), and on November, 23, 1980 ($M = 6.9$). The 1980 earthquake, which killed about 3000 people in a vast area of Southern Apennines, is known as the Irpinia-Basilicata earthquake.

Figure 2 reports a geological map of the zone. The upper conglomerates consist of polygenic pebbles floating into a brown sandy matrix; this material is only slightly cemented and includes thin sandy lenses. The lower “Argille Varicolori” formation consists of highly tectonized gray clay shales. Their typical fabric consists of platy millimetric to centimetric fragments bounded by polished surfaces (Picarelli et al. 2002).

Field surveys, supplemented by data provided by a borehole drilled in the historic centre of the town down to a depth of 151 m, allowed to draw the profile of the conglomerate slab (Figs. 2 and 3). The thickness of this latter is variable: it is higher in the northern and central parts of the platform where it reaches a depth of 115 m (borehole D) and gradually decreases towards South. Some springs located at the bed of the slab indicate the presence of an aquifer.

The geological sections in Fig. 3 show some subvertical fractures crossing the platform, which displays a stepped morphology characterised by some escarpments and by three terraces located at elevations ranging between 825 and 900 m a.s.l. (Fig. 3a). A major escarpment, about 40 m high, subdivides the town into two parts: the historic downtown (located in the northern sector) and the more recent urban centre located on the highest terrace (southern sector). According to Crescenti et al. (1984), the major escarpment might bound a South-North ancient landslide.

As a result of erosion, the boundaries of the platform are subjected to shallow landslides, which generally have their toe into the basal fine-grained deposit. The consequence of these phenomena is a progressive irregular thinning of the hill top, especially in the northern sector (Figs. 2 and 7). The main landslides are shown in Figs. 2 and 3. Figure 4 shows the effects of landslides involving the platform.

The map in Fig. 5 summarises the main geomorphological data including the zones of the town that are subjected to retrogressive landslides, the main cracks on pavements and the presumable direction of slope movements. The figure shows that some damaged buildings are located in retrogression sectors of landslides having the toe in the basal formation. However, even internal zones present

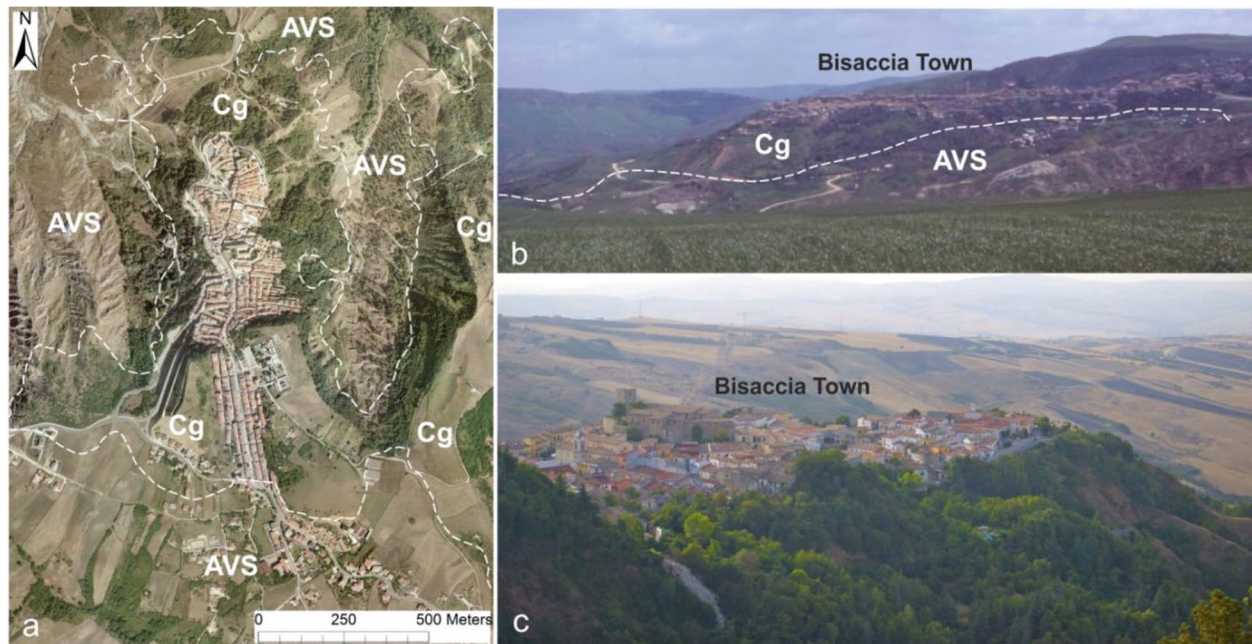


Fig. 1 The Bisaccia hill: **a** orthophoto, **b** the Western and **c** the North-Eastern hillslope. Cg Poligenic conglomerates within a sandy matrix (Pliocene); AVS “Argille Varicolori” formation (Miocene-Oligocene)

sharp changes in ground surface elevation, fractures in roads pavements and extensive damage on buildings, which testify a complex slope deformation process.

As mentioned above, the platform is subjected to extremely slow movements with an important vertical component that is documented in the following. This is testified by continuous extensive damage to the majority of buildings and artefacts, including the farthest ones from the sides of the slab. Based on the recent updated Varnes classification of landslides proposed by Hungr et al. (2014), the overall platform movement that was initially recognized as a “spread” (Picarelli 2000) or as a deep-seated gravitational slope deformation (Di Martire et al. 2016), might be classified as “slope deformation”, a class including complex phenomena that could not be easily assigned to one of the previously defined categories (Varnes 1978) due to their complexity and to the absence of a simple and clearly recognizable mechanism of failure. Typically, these phenomena represent borderline cases involving large soil masses, sometimes entire relieves that experience extremely slow movements often characterized by the absence of a well-defined persistent rupture surface. In particular, Hungr et al. identify five subtypes: “mountain slope deformation”, “rock slope deformation”, “soil slope deformation”, “soil creep” and “solifluction”. The considered case appears as a soil slope deformation, which is defined as a “deep-seated slow to extremely slow deformation of valley or hill slopes formed of (usually cohesive) soils” (Hungr et al. 2014), which is often indicated also as deep-seated gravitational slope deformation.

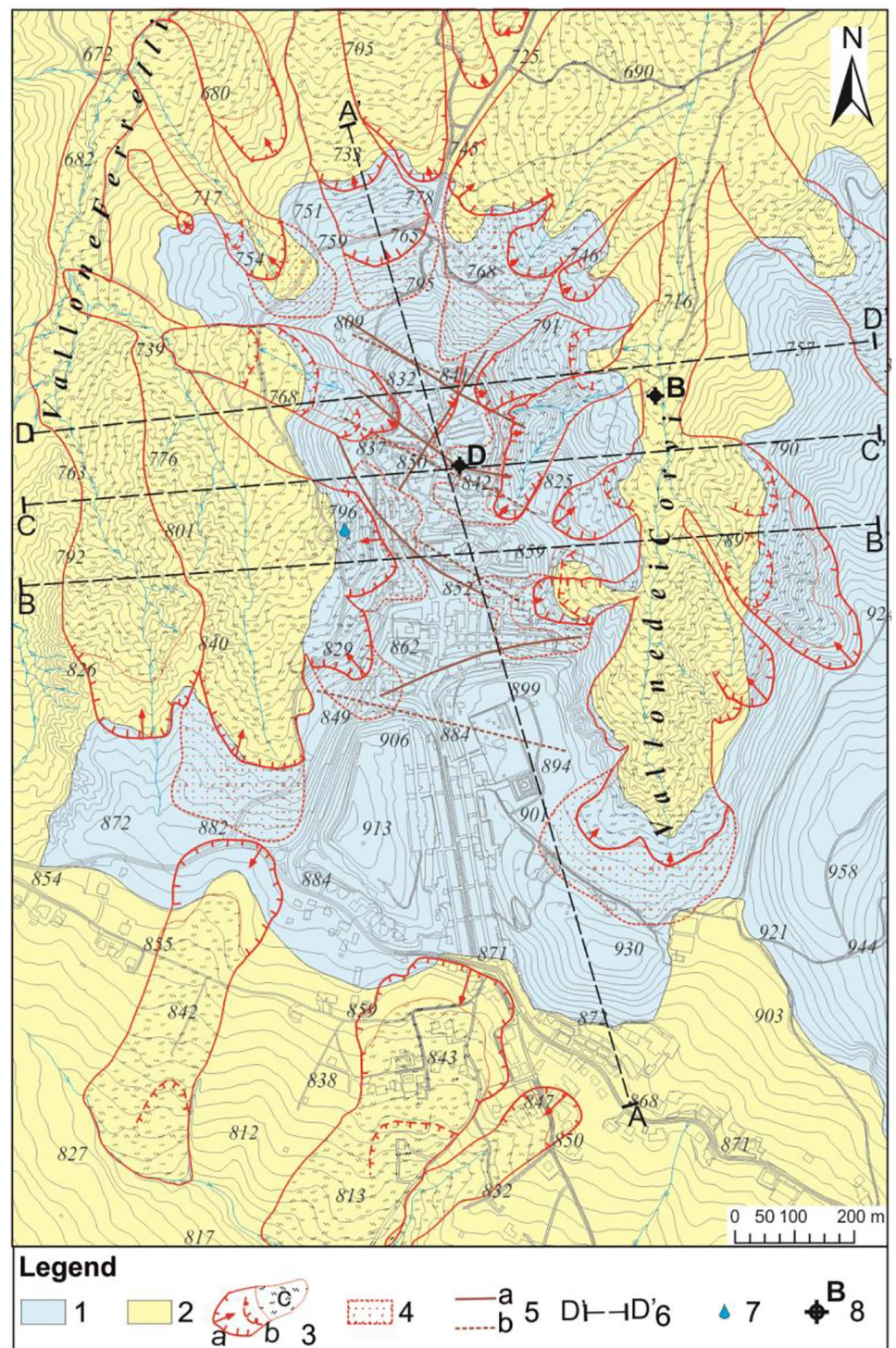
Clay shale properties and groundwater regime

In-depth investigations carried out after the 1980 earthquake allowed collecting a lot of data about the hydraulic and mechanical properties and the groundwater regime in the basal argillaceous formation (Urciuoli 1992; Olivares 1997; Picarelli et al. 2002). This is very deep and consists of highly plastic clay shales with a clay content ranging in the interval 50–70%, a liquidity limit much higher than 100%, locally reaching 200%, and a liquidity index with a minimum value of -0.3.

The mechanical soil behaviour is strictly dependent on fissuring. In triaxial compression tests, the soil behaves as a continuum as far as the deviatoric stress level remains below 20% more or less, then slipping takes place at the contact between soil fragments while a shear surface starts forming connecting adjacent fissures. The failure envelope is curved, being characterised by no cohesion and by a minimum friction angle of 17–18°. Excess pore pressures measured in cyclic undrained triaxial tests are small and positive turning to negative as shear failure is approached (Olivares 1997; Olivares and Picarelli 1999).

For confining stresses around or above the field values, the coefficient of hydraulic conductivity measured by constant head tests in a triaxial cell, is comprised between 10^{-11} and 10^{-12} m/s, a range of values that is quite consistent with the index properties (Picarelli et al. 2002). This suggests that fissures in the field are closed not playing a significant influence on water flow.

Fig. 2 Geological map of the Bisaccia area: 1 poligenic conglomerates with a sandy matrix; 2 “Argille Varicolori” formation; 3 landslide (a main scarp; b minor scarp; c accumulation zone); 4 retrogression sector; 5 major fractures recognized after earthquakes (a 1980 earthquake; b 1930 earthquake); 6 geological cross section (see Fig. 3); 7 spring; 8 borehole



Significant elements about the field pore pressure regime were captured through a set of piezometers. A borehole was drilled in the middle of the Vallone dei Corvi, Eastern valley (site B: Figs. 1a, 2 and 3), where the elevation of the ground surface is around 720 m a.s.l., i.e. about 125 m below the top of the hill in the same cross section (D-D', Fig. 3). Below a few metres deep debris cover, the Argille Varicolori deposit was drilled till a maximum depth of 65 m. Another borehole was drilled in the middle of

the town (site D). In such a section, where the platform is 115 m deep, the conglomerate bed is located 30–40 m above the elevation of the valley floor (Figs. 2 and 3). In the first borehole (site B), three Casagrande piezometers were installed till a depth of 12 m from the ground surface; in addition, five vibrating wire electric probes were located at depths comprised between 7 and 56.8 m. All piezometers were embedded into a sandy filter. The vibrating wire probes installed at depths of 15, 17.5 and 56.8 m

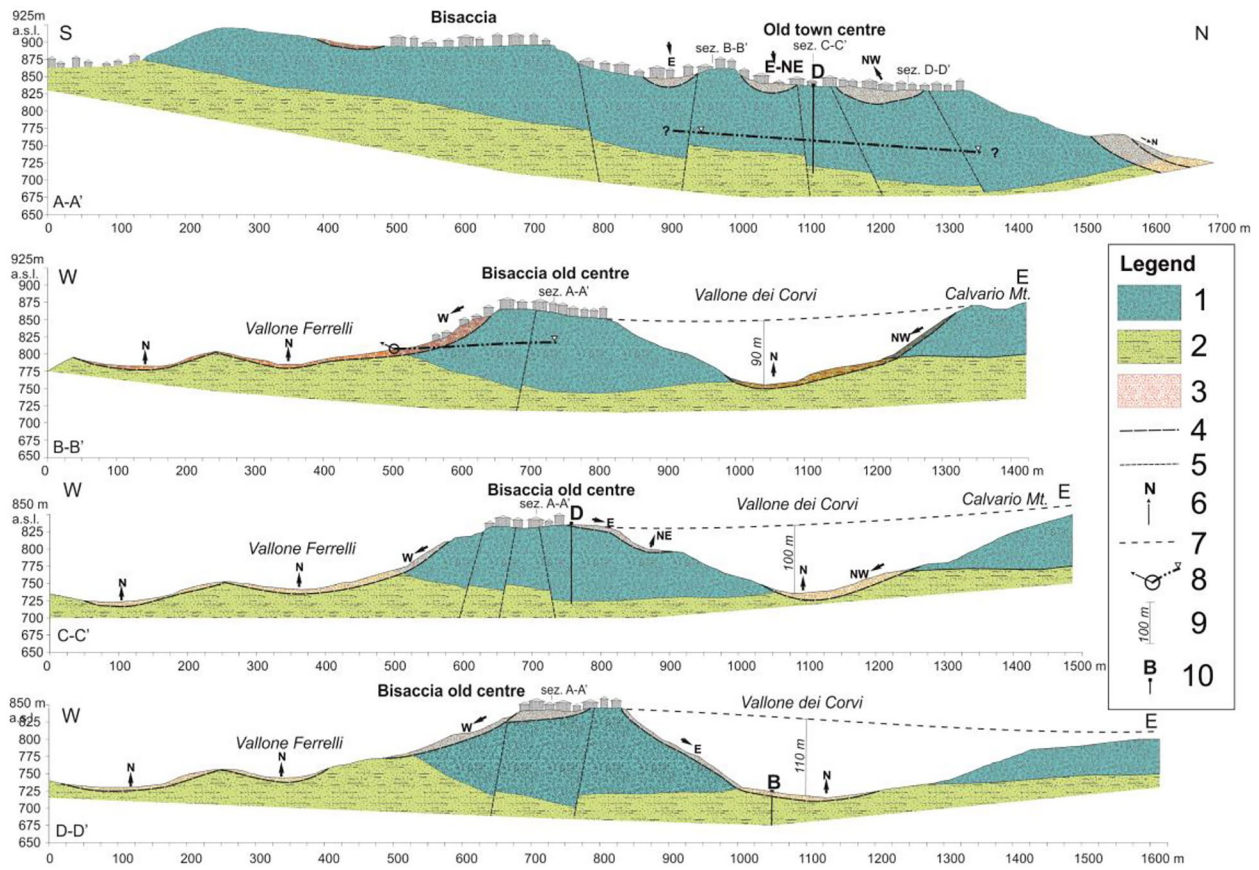


Fig. 3 Geological cross sections of the hill (see Fig. 2): 1 poligenic conglomerates with a sandy matrix; 2 Argille Varicolori formation; 3 accumulation zone; 4 failure surface; 5 major fracture; 6 direction of

landslide movement; 7 presumed original profile of the conglomerate top; 8 spring and water table surface based on data from borehole D; 9 presumed original conglomerate thickness; 10 borehole

soon recorded negative pore pressures, which after a few months dropped to zero remaining nil in all subsequent readings due to an evident cavitation phenomenon into the filter (Picarelli and Urciuoli 1993). It was then decided to install another cell, which was embedded into a clayey filter at a depth of 27.5 m in a parallel

borehole. The results of all readings over a time interval of 2 years are shown in Fig. 6a. All instruments display quite low values. In particular, the pore pressures measured at Casagrande piezometers were positive and less than the presumed steady-state value obtained from the numerical analyses discussed below, while as



Fig. 4 Effects of ongoing slope movements

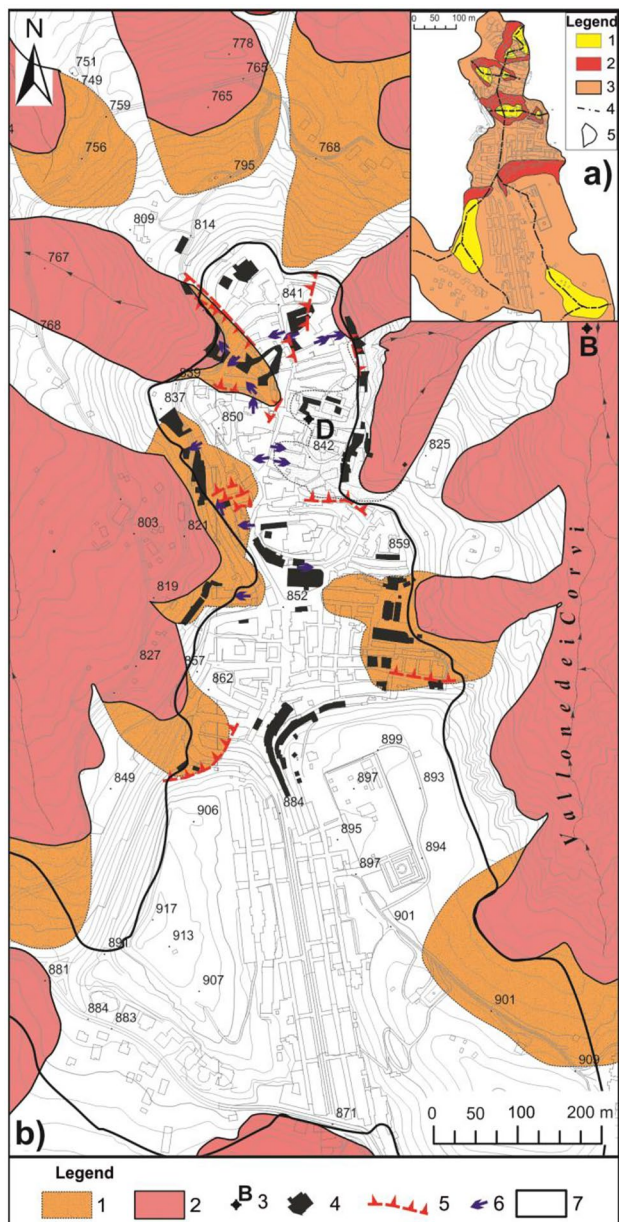


Fig. 5 **a** Geomorphological map: 1 morphological height; 2 escarpment; 3 morphological depression or sub-horizontal surface; 4 watershed; 5 morphological top limit of the hill. **b** Landslide effects: 1 retrogression sector; 2) zone of depletion or accumulation; 3 borehole; 4 heavily damaged building; 5 macro-fracture; 6 presumable displacement vector of surveyed fracture; 7 morphological hilltop

mentioned above, negative values were measured by three deeper vibrating wire cells. Notice that the negative readings reported in the figure are the stable value (around -10 kPa) measured through the last cell at a depth of 27.5 m and those measured before cavitation at the other two cells. In the borehole D located in the town, a Casagrande piezometer was installed at a depth of 95 m within the conglomerate formation, while a vibrating wire

cell was placed in the clay shale deposit at depth of 149.5 m, i.e. 54.5 m below the basal surface of conglomerates. The first piezometer allowed measuring the water level, in the conglomerate slab, 35 m above the top of clay shales (Fig. 6b). Surprisingly, the cell installed in clay shales recorded a continuously decreasing level. In fact, as indicated by the small black arrow in the figure, the pore pressure measured in 1991 (i.e. 11 years after the 1980 earthquake), which is quite higher than the presumed value calculated for steady-state conditions (dotted line), in the following years progressively decreased below the steady-state value.

A steadily ongoing general deformation process

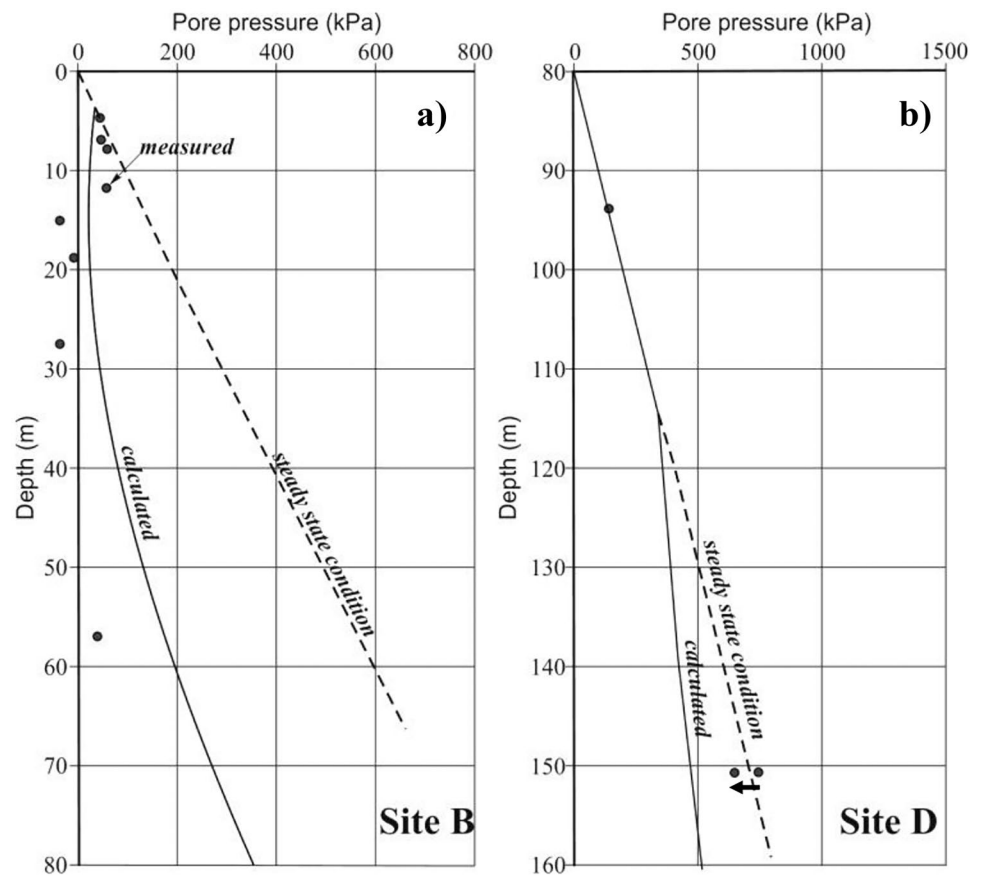
Main effects of the 1980 earthquake and hill deformation until 1988

On November, 1980, a wide area of Southern Italy was shaken by a strong seism ($M = 6.9$), the so-called Irpinia-Basilicata earthquake. As a result, long cracks appeared on pavements of the town, and a number of buildings were damaged even though no casualties were recorded. It was soon evident that the most severely damaged buildings were all located in vicinity of the cracks (Fig. 7).

Based on historic data, the most recent strong earthquakes in the same area lead back to 1694, 1732, 1851, 1910 and 1930 (Boschi et al. 1995). All events caused a limited number of casualties, but in all cases, the damage to buildings, walls and pavements was relevant. The consequences of the 1930 earthquake, which caused eighteen victims, are described by Oddone (1930) and by Alfano (1931), who mention cracks on pavements; based on their descriptions, the cracks have been plotted in Fig. 7. Interestingly, the main effects of the 1930 and 1980 earthquakes appear to be very similar. These and further elements, such as earlier escarpments (indicated in the figure as morphological steps), which are overcome by old staircases, suggest the recurrence of similar repeated deformation mechanisms that are probably caused by movements of single conglomerate blocks triggered by shaking.

The inferred deformation mechanisms suggested performing some targeted investigations. In fact, in February, 1981, thus 4 months after the quake, a number of benchmarks were installed in the downtown. Topographic readings were then carried out in the months and in the years after. Vertical displacements measured at benchmarks located along the South-North axis of the hill in February, 1982, and in October, 1988, are shown in Fig. 8. These highlighted the development of a subsidence process characterized by increasing settlements in the South-North direction. The figure also shows that each displacement profile could be easily subdivided into a series of segments, which suggest independent movements of single blocks; while some of them seem to display nearly vertical displacements, others seem to tilt while settling. This is consistent with the fact that the main discontinuities in the displacement profile closely correspond to fractures in the pavements, indicated with arrows in the lower plot. A further interesting remark is for the very similar shape of the vertical displacement plots and of the hilltop profile that is magnified in the same figure, as this last was just the result of continuing hill subsidence started long time before (Fenelli et al. 1992).

Fig. 6 Pore water pressures measured below the Vallone dei Corvi bed (a) and below the conglomerate platform (b), compared to results of numerical simulations (after Di Nocera et al. 1995)



Movements of the hill since 1992

The 1988 topographic readings are the last on site record of ground movements. However, the availability of satellite images since 1992 allowed collecting further useful data. Satellite PSInSAR data are available from the ERS (1992–2000), Envisat (2003–2010) and COSMO-Sky Med (2011–2013) sensors, this latter being referred as CSK. Such data were processed within the PST-A, a high-precision plan of remote sensing provided by the Italian Ministry of the Environment (Costantini et al. 2017). By integrating the results of previous topographic readings, an almost continuous temporal reconstruction of hill movements from 1981 until the end of 2013 has been obtained, with a “black hole” in the interval 1988–1992 and further smaller gaps in the periods 2001–2003 and 2010–2011.

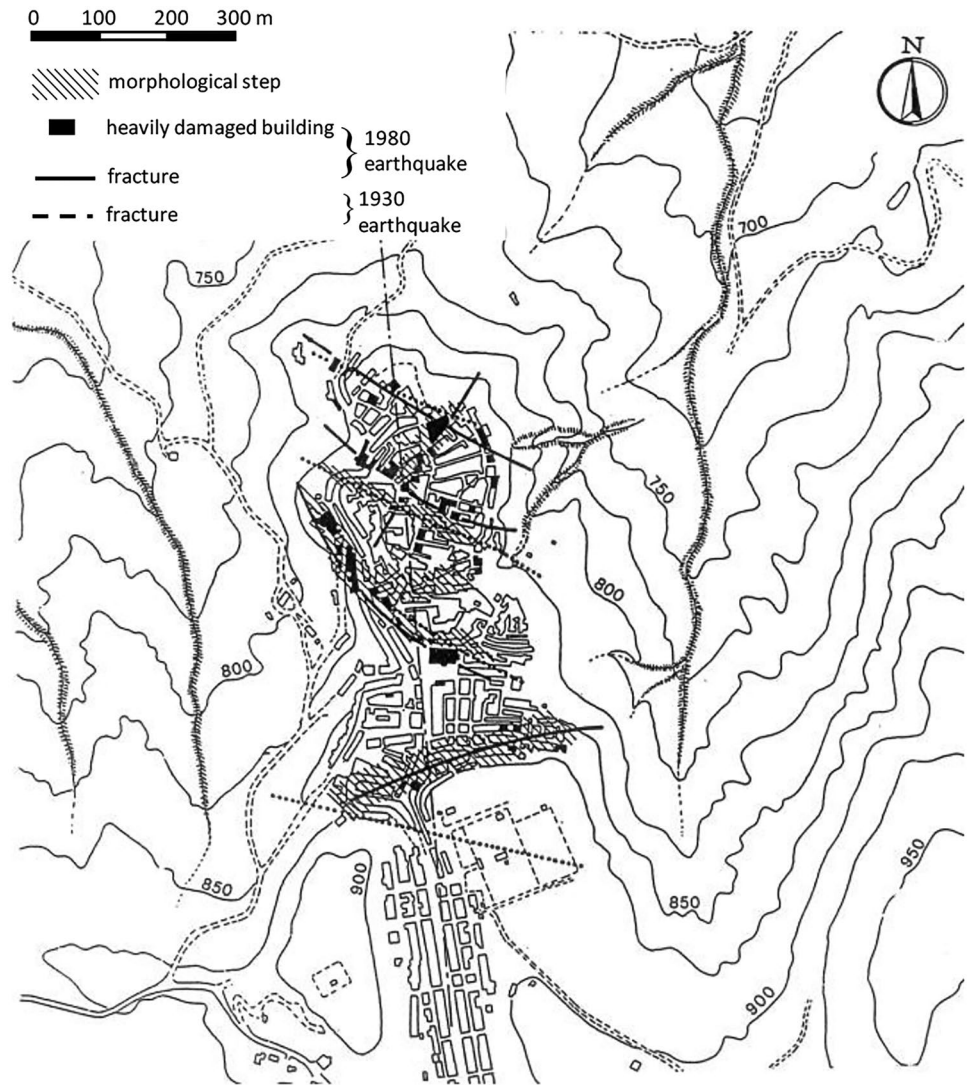
As it is well known, interferometric processing of satellite images provides the displacement component along the satellite line of sight (LOS), whose direction in the study area is close to the W-E direction. Therefore, in the case at hand, satellite displacement monitoring is much more sensible to the vertical and West–East components than to the North–South one (e.g. Di Maio et al. 2018; Di Traglia et al. 2021; Vassallo et al. 2021). Within the PST-A plan, ERS (1992–2000) and Envisat (2003–2010) series were processed for both descending and ascending passes of the satellite, while the CSK series (2011–2013) was processed only for the descending pass.

Figure 9 reports the available data in terms of average yearly displacement rate along the LOS. A significant number of scatterers was detected on the buildings of the town, with increasing density of targets moving from ERS to Envisat and then to CSK. LOS displacement rates generally increase from South to North reaching at the northern edge of the town values in the order of 1–2 cm/year, which are quite consistent with topographic readings (Fig. 8). In Fig. 9, the white squares are used to indicate the buildings for which both ascending and descending pass data are available.

The readings by spaceborne InSAR are one-dimensional measurements that come from the projection, along the radar LOS, of vertical, West–East and South–North displacement components. According to De Luca et al. (2017) and Di Traglia et al. (2021), data detected from three different LOS directions on common pixels would therefore be necessary to obtain the three components of ground displacement. In the case at hand, for which information is available for two LOS directions only, the vertical and the West–East components of displacements (s) or average rates (v) were estimated from the available ascending and descending pass data relative to ERS and Envisat sensors through the following equations:

$$v_U \cong \frac{v_{asc} + v_{desc}}{2 \cos \theta} \quad (1)$$

Fig. 7 Main damages caused by the 1930 and 1980 earthquakes (Fenelli et al. 1992)



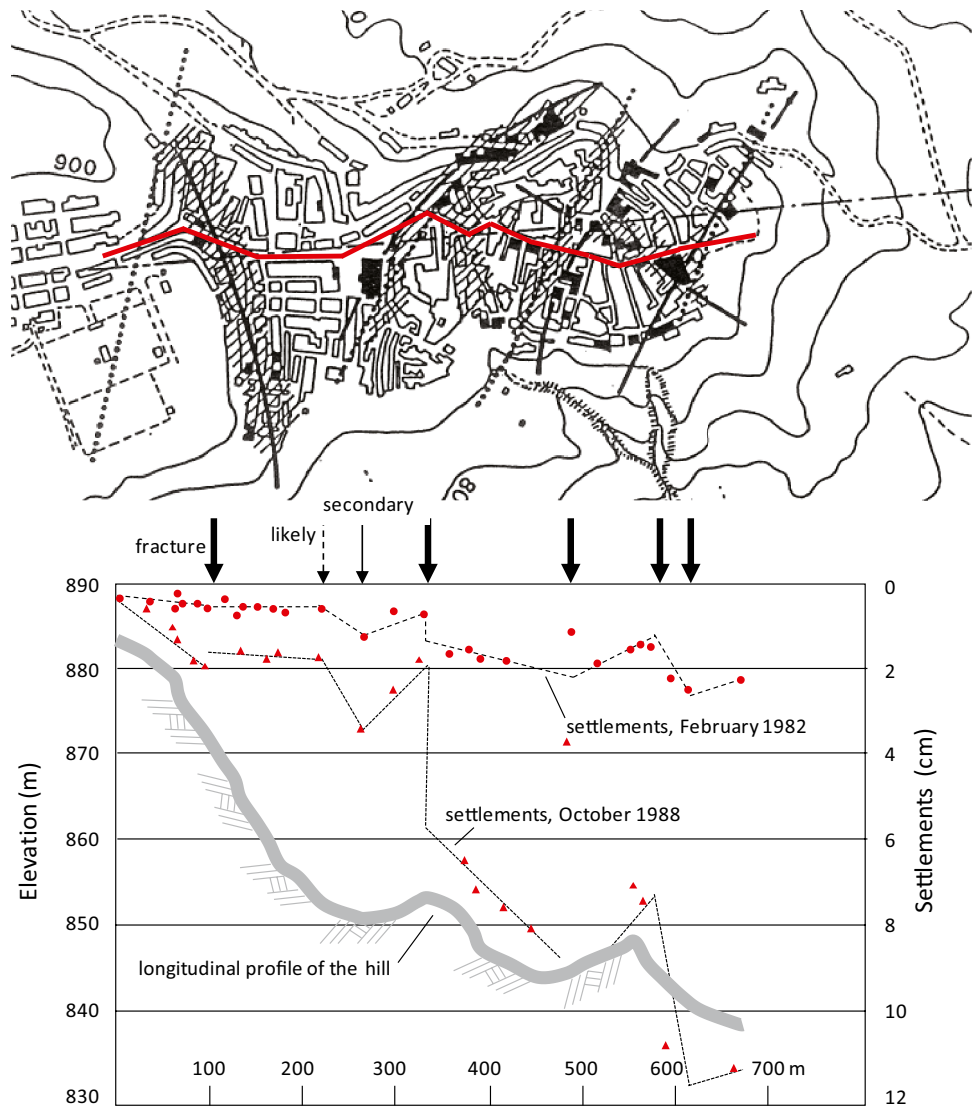
$$v_E = \frac{v_{desc} - v_{asc}}{2 \sin \theta \cos \alpha} \quad (2)$$

where $\theta = 23^\circ$ is the look angle, i.e. the angle between the LOS and the vertical, and α ($= -11^\circ$ on ascending orbit, and $= 180^\circ + 11^\circ$ on descending orbit) is the satellite heading angle, i.e. the angle between the projection of the sensor path on the ground and North (Fig. 9a). Negative values of v_V indicate downward movements, while negative values of v_E correspond to westward movements. It is however worth to mention that the former equation is approximate, since it neglects the contribution along the LOS of the North–South component of displacement compared to that of the vertical component. This is justified by the fact that the LOS projection on the ground forms a small angle ($\pm 11^\circ$) with the West–East direction.

Figure 10 shows the elaboration of data for the 2003–2010 time interval (Envisat). Ascending and descending displacement rates reported in Fig. 9d–e were averaged on $50 \text{ m} \times 50 \text{ m}$ pixels and then processed using Eqs. (1) and (2) so as to obtain raster maps in the vertical and West–East directions. Vertical rates range between -3 and -19 mm/year . Similar values (0 – 16 mm/year) are

estimated for the horizontal components in the E–W direction, which point to East or to West depending on the zone, with a prevalence of eastward displacements. The moduli of vertical displacement rates clearly increase moving from South to North with a significant step through the cross section located at an elevation of about 885 m , where is present the high escarpment mentioned above, which might bound an ancient landslide. The highest values of the E–W rate are observed in the northern sector and, locally, in the vicinity of hillslopes. LOS displacement rates for the descending CSK orbit (Fig. 9f) seem to confirm that the values increase in proximity of scarps and retrogression sectors. As mentioned above, available data do not allow obtaining reliable information about the South–North component of displacements, i.e. in the direction of the longitudinal hill axis. In any case, the entire set of data highlights an active deformation process of the entire platform possibly including local effects along its contour. Based on a rough review of data concerning other towns in the same area, the examined case appears to be a unique situation (Di Marino 2011).

Fig. 8 Vertical displacements measured along the main axis of the downtown between February, 1981, and October, 1988 (redrawn after Fenelli et al. 1992)

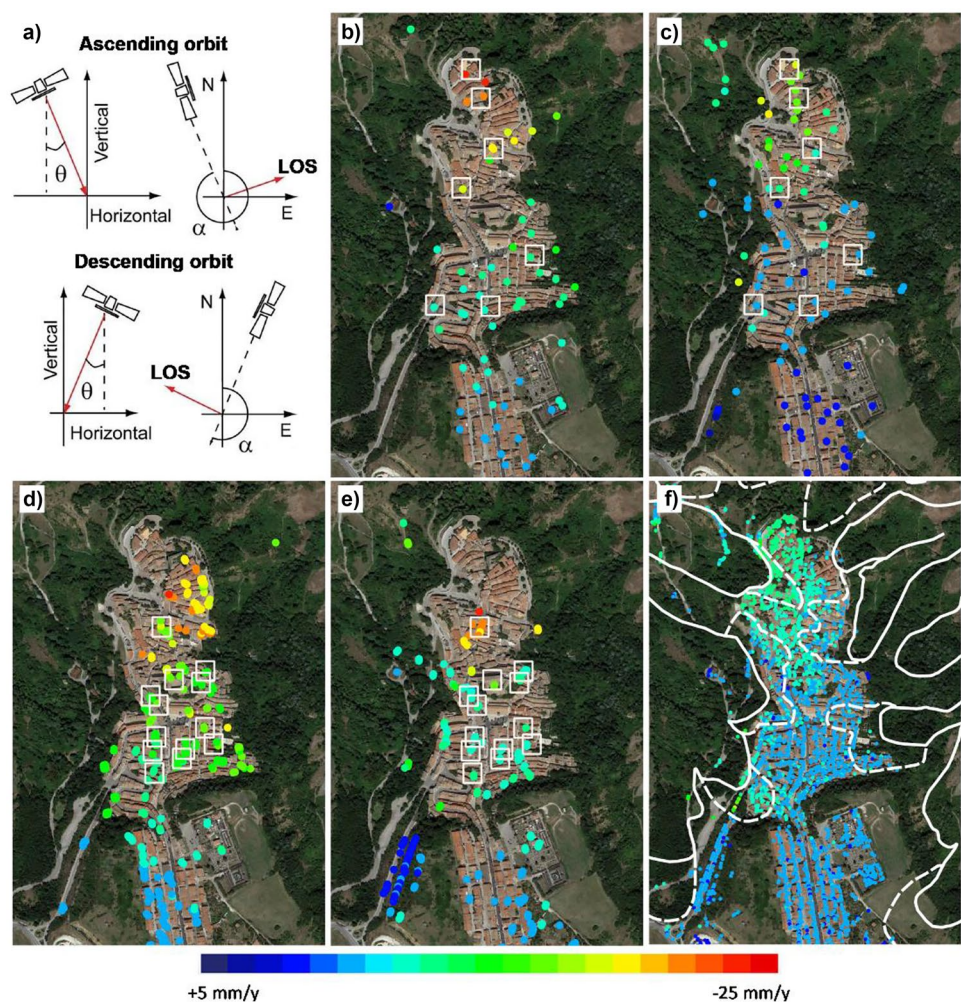


To further deepen the subject, Fig. 11 shows vertical and West–East displacements of a number of representative buildings for which data are available for both ascending and descending satellite passes in different time intervals. Such an information can be considered more accurate than that provided by Fig. 10, being the data related to specific buildings rather than averaged on wider areas although, of course, more discontinuous in space. For CSK satellite data (2011–2013), since only descending orbit data are available, vertical and W–E displacements were obtained under the hypothesis that their ratio is equal to that obtained in the Envisat monitoring period 2003–2010. The displacement field appears consistent over the entire 20 years observation period (1992–2013), with some evident rate changes in time. For instance, in the zone of buildings Q and R, which are quite close to each other, higher vertical displacement rates have been recorded in the period 2003–2007 than in the interval 1992–2003. On the other hand, if the whole monitoring period is considered,

displacement rates globally seem to decrease with time in the entire built area. The trend of horizontal displacements in the W–E direction appears more complex, with more evident variations in the average yearly rate in some zones than in others, and an apparent change of sign in the zone of buildings Q and R.

An updated profile of vertical displacements in the South–North hill axis is plotted in Fig. 12 where it is again compared to the platform profile. As a first useful consideration, the trend of recent readings is fully consistent with the previous one. The figure also shows the cumulative 1981–2013 displacements obtained by summing the data from satellite images to those obtained from topographic readings (Fig. 8), integrated with extrapolated values that cover the “black holes” in the time intervals 1988–1992, 2001–2003 and 2010–2011. The obtained plot again suggests a long-lasting deformation process, presumably started well before the 1980 earthquake and characterized by apparently independent movements of single blocks, which led to the present platform profile. The peak

Fig. 9 a) Schemes of InSAR reference geometries on ascending and descending orbits (mod. from Di Traglia et al. 2021); LOS average displacement rates (superimposed to a Google Earth view-Landsat/Copernicus image) from: ERS ascending **b)** and descending **c)** orbits (1992–2000); Envisat ascending **d)** and descending **e)** orbits (2003–2010); CSK descending orbit **f)** (2011–2013). A negative value indicates that the scatterer is moving away from the sensor. White squares in **b), c), d), e)** show buildings for which both ascending and descending data are available. Landslide contours (Fig. 2) also reported in **f)**



settlement value from 1981 to 2013, just at the northern boundary of the platform, is approximately 70 cm, which corresponds to a rate a little higher than 2 cm/year.

Interpretation of the observed deformation phenomena

Considering that all readings obtained from satellite images are in line with those provided by topographic measurements, the set of all available data, which globally covers quite a long time interval (about 32 years, from 1981 to 2013), forms a clear and consistent framework. They testify that the hill is subjected to continuing deformations with a significant vertical component and lateral movements in the direction normal to its axis; unfortunately, no information is available about the displacement component in the axis direction. In particular, the vertical displacement profile in the South-North direction (Fig. 12) suggests that the platform consists of distinct blocks that subside into the bedrock with a rate that increases moving from South to North. The most recent data show that it is now slowly decreasing (Fig. 11).

In the considered time interval, the highest vertical displacement rate, measured at the northern edge, is not far from 2.5 cm/year, while it is extremely small (or nil) at the southern edge behind

the high escarpment that separates the oldest centre from the newest part of the town. The maximum cumulative vertical displacement over the investigated time interval of 32 years has been about 70 cm. The horizontal movement rate along the West–East direction is not negligible as well, ranging from less than 2 cm/year to almost zero depending on monitored area; with the exception of small zones of the platform, it essentially develops in the West–East direction. Considering the long time interval covered by available data and the vertical displacement profile that is very similar to the shape of the ground surface, the described deformation history appears to be only the present stage of a process that has begun long before.

The effects of such phenomena are evident. In fact, the morphological steps present in the town are likely to be an effect of movements of conglomerate blocks. Moreover, although in the years after the 1980 earthquake part of the damaged buildings was demolished and rebuilt and part has been repaired, day by day, pre-existing cracks are widening, and new cracks are opening in old and new buildings, on walls and pavements, while some buildings are clearly tilting.

Such a complete and consistent data base, supported by the results of laboratory tests and of pore pressure monitoring, has

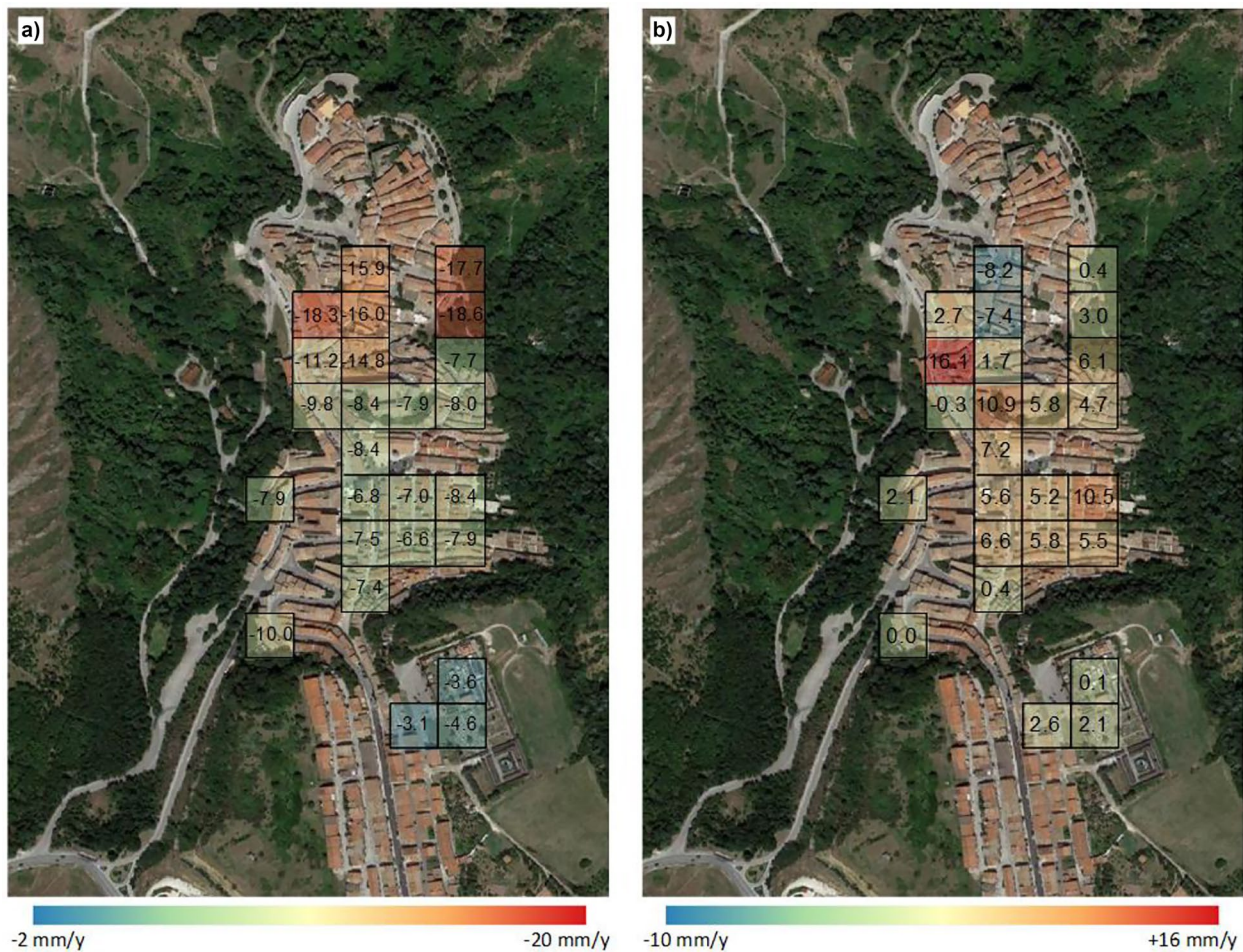


Fig. 10 Average displacement rates in the period 2003–2010 in the vertical **a)** and West–East **b)** directions obtained from Envisat satellite data, superimposed to a Google Earth view-Landsat/Copernicus

image (negative rates correspond to downward and westward displacements; positive values correspond to eastward displacements)

been a useful tool for a mechanical interpretation of ongoing phenomena. Based on a careful evaluation and analysis of all data, a major factor is probably the intense erosion process that is deepening both valley floors; a significant role seems also to be played by periodic earthquakes that shake the area; finally, the landslides that have indented and still erode the lateral sides of the hill represent another active factor.

Based on geological data, erosion is supposed to have started about 300,000 years ago along two parallel faults more or less corresponding to the axes of the lateral valleys. Figure 13 schematically reports the geological evolution of the area. Such a process was simulated through a 2D FEM numerical analysis (Picarelli and Urciuoli, 1993). The initial top of conglomerates was assumed to be horizontal, and then these were gradually removed in order to reproduce the present morphology of the area. The rate of conglomerate erosion was considered to be either constant or variable assuming a threefold increase after complete dismantling of the slab in order to account for the different erodibility of conglomerates and of clay shales. The groundwater table was initially located at the top of clay shales, then, after removal of the uppermost conglomerate layer, it

was gradually lowered following the deepening of the valley floor. The main vertical cracks in the platform were reproduced by thin (30 cm) vertical deformable elements; finally, an interface allowing horizontal relative displacements was located at the contact between the platform and the bedrock. The conglomerate slab was simulated as a linear elastic medium while the clay shale behaviour was reproduced through the Cam Clay model adopting the soil parameters obtained by a rich campaign of laboratory tests.

The main result of the analysis was a strong and delayed swelling of the valley floors (a in Fig. 14) and some sinking of the hill within the basal formation (b in Fig. 14) due to the combined effect of unloading caused by erosion and both high deformability and low permeability of clay shales (Urciuoli 1992; Picarelli et al. 2002). Another important output was some lateral spreading of the hill due to decrease of the lateral confinement; in particular, the analysis suggests the formation of a shear zone at the top of the basal formation (c and d in Fig. 14). Some clues about that might be provided by the water content profiles of clay shales (Fig. 15) obtained from measurements on samples taken from the boreholes B and D, compared to the values calculated through the numerical analysis

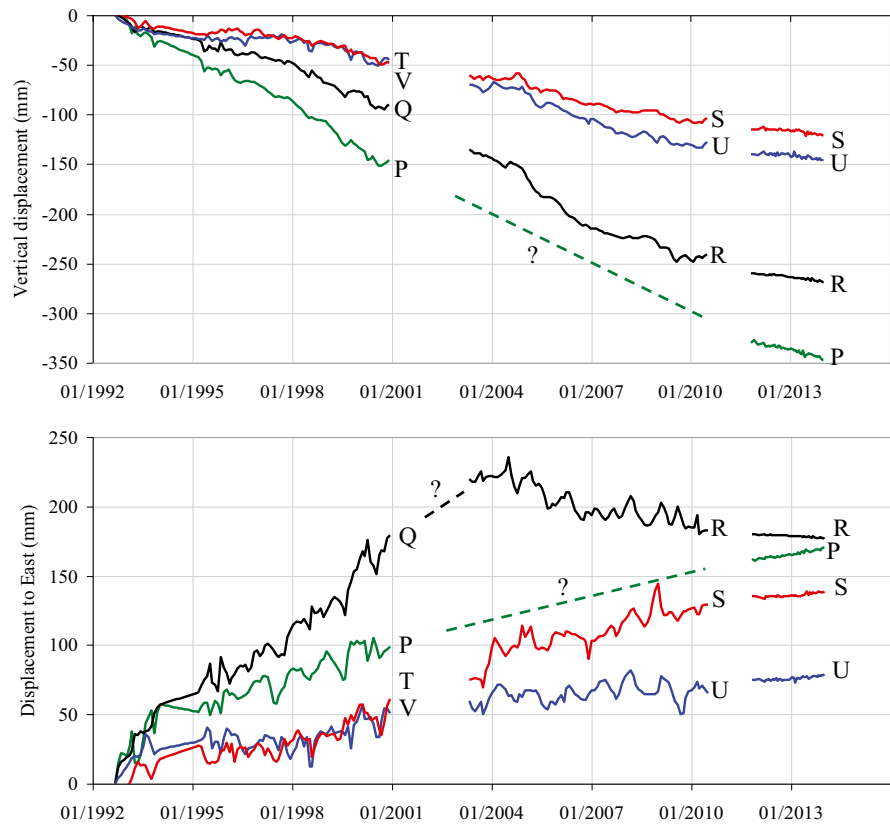


Fig. 11 Time series, for a number of buildings, of vertical displacement (negative if directed downwards) and displacement to East, obtained from satellite ERS, Envisat and CSK data

Fig. 12 Summary of data available about vertical displacements along the main axis of the downtown: topographic readings (1981–1982; 1982–1988); satellite images (1992–2000; 2003–2010; 2011–2013); total (1981–2013)

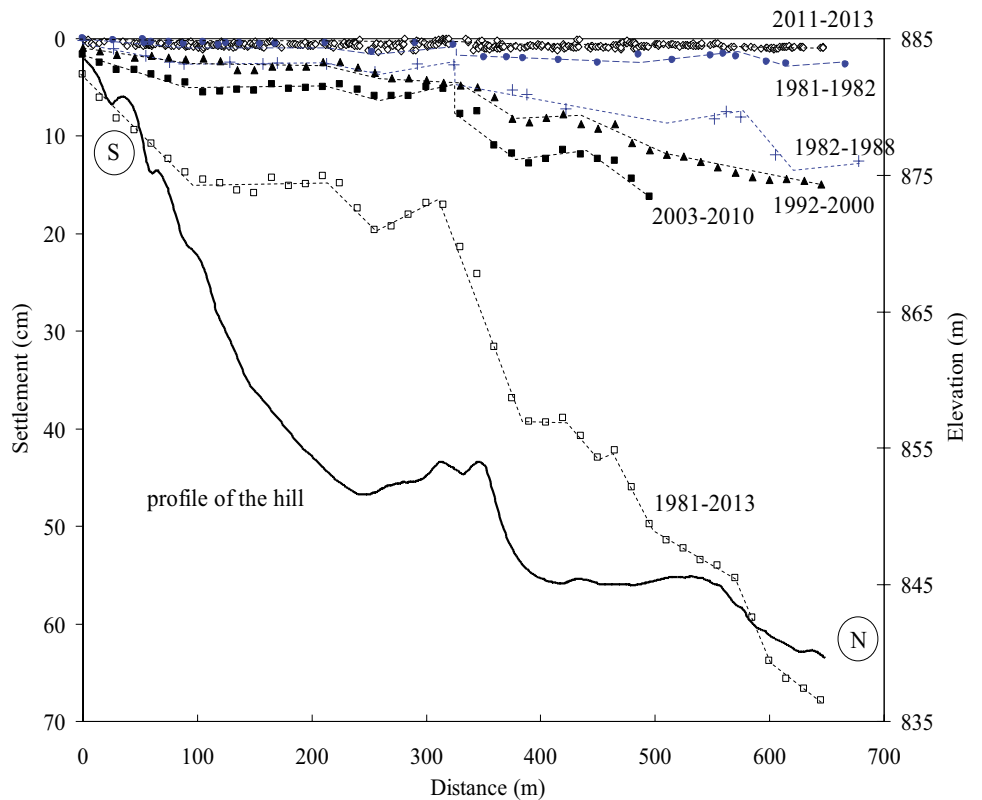
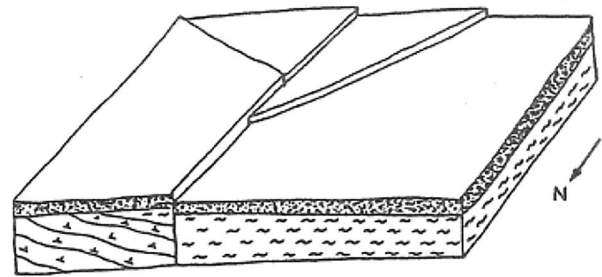
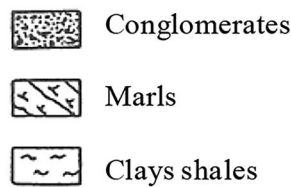
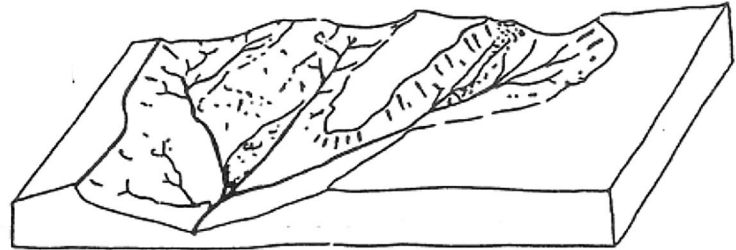


Fig. 13 Evolution of the Bisaccia area (after Di Nocera et al. 1995)

7-300.000 Y.B.P



18000 Y.B.P



BISACCIA

PRESENT



(Picarelli and Urciuoli 1993). In particular, while these last can capture the trend of the water content profile along the vertical B, they underestimate the water contents measured within a depth of about 15 m under the platform. This might just indicate the presence of a thick shear zone generated by the process of lateral spreading discussed above.

Figure 16a shows the calculated deformation of a cross section of the platform. In particular, it shows that the lateral blocks are subjected to some rotation, which implies a distortion of the slab and formation of a concave interface at the conglomerate-clay shale contact. The figure also suggests the development of tensile stresses at the base of the platform, which might lead to formation of further vertical cracks. Interestingly, a similar deformation field as in Fig. 16a has been observed in some Canadian river valleys indented in highly plastic clay shales (Fig. 16c).

All these results are consistent with the general framework provided by field surveys and by monitoring, depicting in a convincing way the deformation process of the platform. Figure 16a, in particular, clearly shows the mechanism of sinking of conglomerate blocks in the bedrock (see also Fig. 16b). Also, a careful consideration of

Fig. 16a could explain the observed horizontal movements in the East–West direction as a result of the combined effect of lateral spreading and of tilting of blocks that is confirmed by the tilting of some buildings (Di Marino 2011); in particular, a clockwise or anti-clockwise rotation can justify westward or eastward movements. It also justifies the presence a deep aquifer above the deformed concave top of the bedrock under conglomerates as shown by piezometer readings in borehole D (Fig. 6b). Finally, the analysis allows explaining the deficient pore pressure field measured in the subsoil of the eastern valley (borehole B, Fig. 6a). In fact, due to the low permeability and high depth of the fine-grained bedrock, the erosion rate is quick enough to generate a constant deficient pore pressure regime within a deep zone under the valleys bed (Koppula and Morgenstern 1984; Fenelli and Picarelli 1990). Such a pore pressure regime seems to play a significant role on the stability of the hillslopes. In fact, accounting for the low shear strength of clay shales, a steady-state pore pressure profile (as in Fig. 6) would imply the triggering of deep landslides favoured by the presence of vertical fractures in the conglomerate slab. Under this condition, the platform should have been completely dismantled by landsliding since long time. Instead, due to

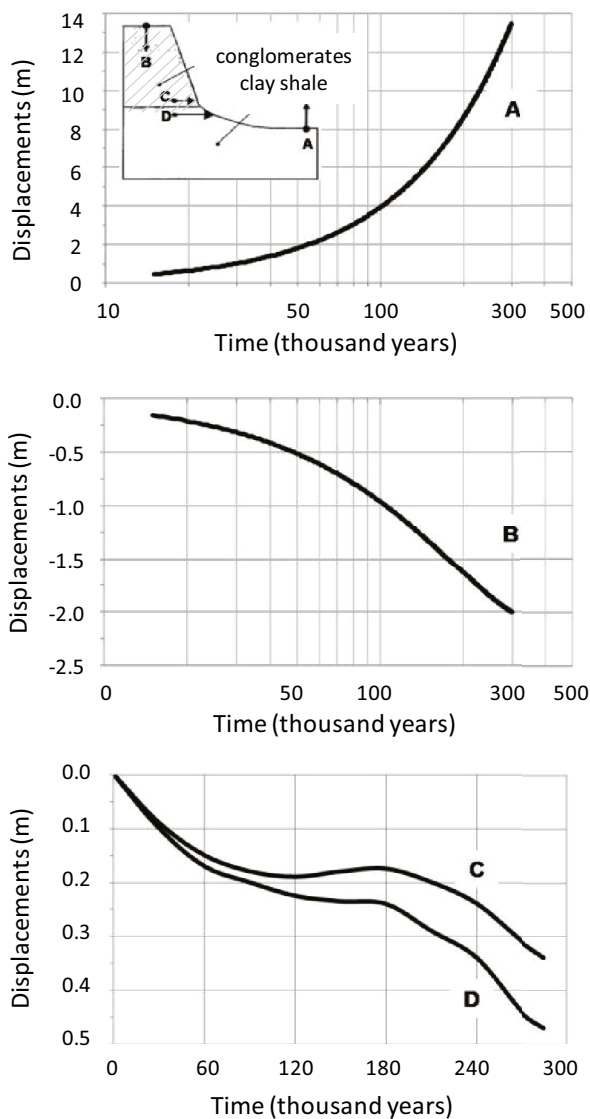


Fig. 14 Calculated time-dependent swelling of the centre of the valley's bed (A), settlement of the hill (B) and horizontal displacements of conglomerate bed (C) and clay shale top (D) (Urciuoli 1992)

the deficient pore pressure regime, the shear strength of clay shales is high enough to assure a safety factor higher than one (Di Nocera et al. 1995). Not for nothing, the landslides that have been recognized along the hill contour consist of large blocks with a small toe in clay shales, thus involving only the shallowest part of the basal formation where pore pressures are less affected by erosion.

Strong earthquakes, which in the area at hand have a return time of some tens of years, certainly play some role on the soil slope deformation process. This was a sound hypothesis when, just after the 1980 earthquake, Bisaccia became the focus of specific investigations. The general continuing deformation of the hill

was in fact considered to be the clue of a process of post-seismic subsidence consequent to the building up of positive excess pore pressures induced by the shock (Fenelli et al. 1992; Olivares 1997; Silvestri 1997). Specific investigations on the subject supported by special cyclic triaxial tests on undisturbed specimens and by numerical analyses confirmed the reliability of such a hypothesis (Lampitiello et al. 2001; Olivares and Silvestri 2001). In particular, the seismic interaction between the conglomerate slab and the underlying clay shales was investigated through targeted analyses carried out by interpreting the 1980 seismic motion measured by an accelerometer located just in the town of Bisaccia and soil parameters obtained through targeted laboratory tests (Olivares 1997). Based on those analyses, during the earthquake quite a large soil volume under the slab should have experienced positive excess pore pressures triggered by the cyclic shear stresses induced by the seism and favoured by the strong contrast in stiffness between clay shales and conglomerates (Fig. 17). The high initial pore pressure and the decreasing value measured in the time interval 1991–1996 at a depth of 151 m, just under the platform (Fig. 6b), might testify a post-seismic consolidation process (Fenelli et al. 1992).

The temporal evolution of vertical displacements of the platform since February, 1981, until 2013 (thus ignoring the deformation cumulated in the time interval between November, 1980, and February, 1981) can be obtained coupling the readings obtained by topographic measurements and satellite data. A plot of settlements at site D in the northern sector of the town is shown in Fig. 18. In the same figure are reported the results of numerical analyses based on the results of laboratory tests on natural samples (Lampitiello et al. 2001), in the assumption of 2D dissipation of the calculated excess pore pressures triggered by the 1980 earthquake. The evolution of the settlement rate is characterized by a typical decreasing trend, even though the monitored displacement is higher than the predicted one well before the availability of satellite images. Such a difference might be explained by the presence of a thick compressible shear zone. These considerations suggest that any strong earthquake occurring in the area at hand can lead to similar effects contributing to the ongoing deformation process.

Finally, some role in the observed displacement field is probably played by the landslides that erode the lateral slab sides. Such effects, which might be testified by some higher than the average horizontal West–East displacement values provided by satellite images, are of course limited to the unstable zones.

As outlined above, unfortunately, no data are available about the horizontal displacement component in the South–North direction. Such an information might be useful to complete the described general framework. In this regard, the Authors believe that some significant movement might be taking place also in such a direction, favoured by the morphology of the entire area, which leans just in the South–North direction. In particular, the hypothesis by Crescenti et al. (1984) that the platform is cut by the scarp of an ancient landslide suggests that the described slope deformation process might be influenced also by the presence of a deep slip surface.

Fig. 15 Measured and calculated water content profiles in the subsoil of eastern valley (**site B**) and under the conglomerate bed (**site D**) (redrawn after Picarelli and Urciuoli 1993)

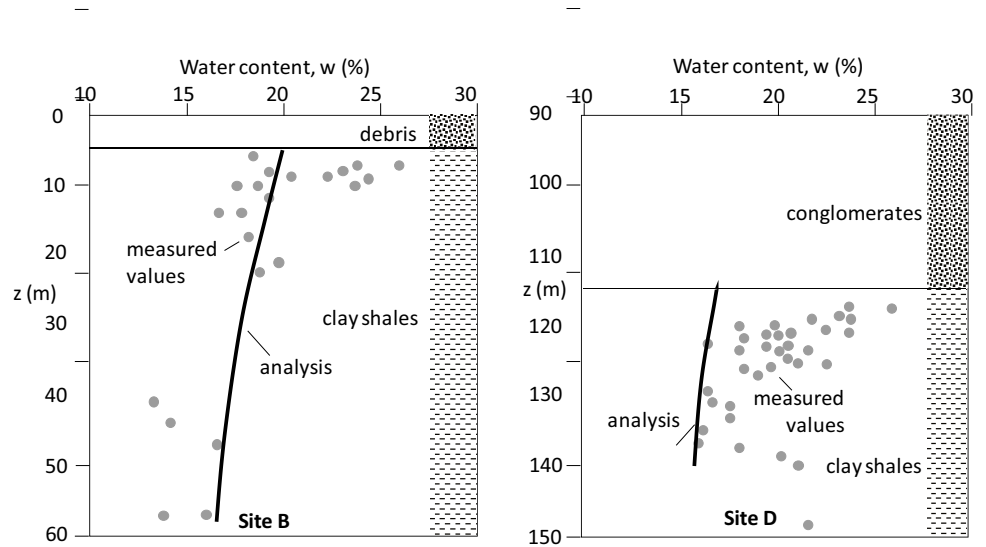
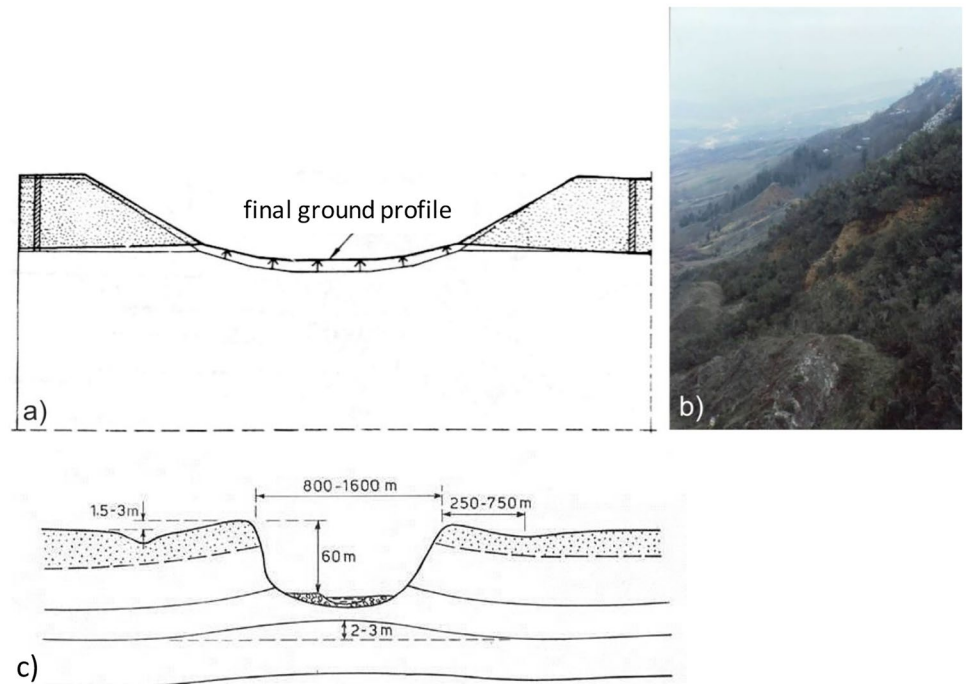


Fig. 16 a) Simplified cross section of the Bisaccia hill and displacement vectors obtained from numerical analysis (Picarelli and Urciuoli 1993); **b)** the Eastern Bisaccia hillslope that is sinking in the clay shale deposit; **c)** effects of erosion in the Saskatchewan river valley (Matheson and Thomson 1973).



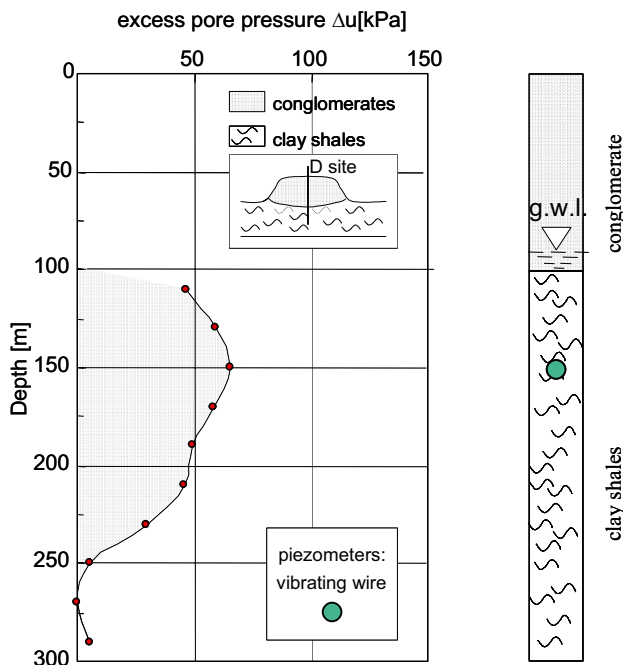
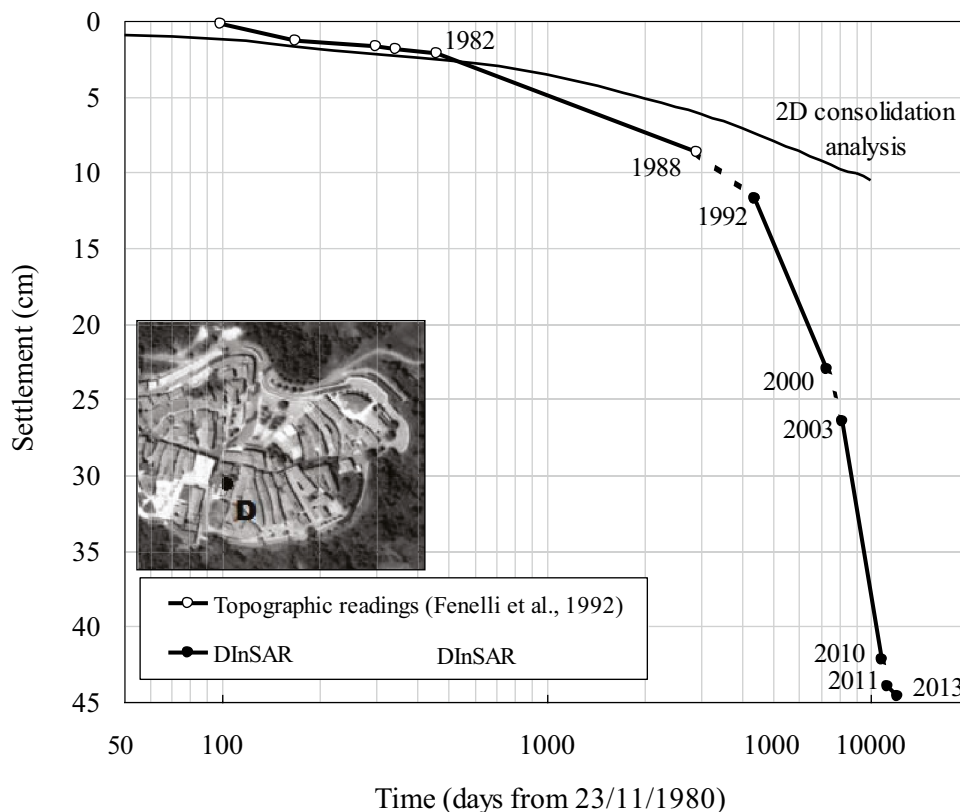


Fig. 17 Calculated excess pore pressures induced by the Irpinia-Basilicata earthquake (Olivares and Silvestri 2001)

Fig. 18 Temporal evolution of the vertical displacement at point D based on both topographic readings and satellite images compared to calculated post-seismic consolidation (modified after Lampitiello et al. 2001)



Summary and conclusions

The old town of Bisaccia rises on a thick elongated conglomerate platform that overlies a deep deposit of highly plastic clay shales. After the strong 1980 Irpinia-Basilicata earthquake, some in-depth field and laboratory investigations were carried out in order to recognize the effects of the event in the town. In particular, the results of topographic readings carried out in the period 1981–1988 brought to light a general deformation mechanism of the hill. Numerical analyses were then carried out to interpret the effects of either erosion that is modelling the area where the platform rises either seismicity. The availability of satellite images since 1992 has then allowed to keep track of the movements occurred in the subsequent years providing an important and consistent framework that helps in the definition of a comprehensive scenario of the geomorphological phenomena that affect the area.

The hill is an about 1.5 km long fractured conglomerate platform with an irregular contour created by some shallow lateral landslides that are eroding the hillslopes. The conglomerate blocks are slowly sinking into clay shales. Available satellite image data bring to light also a horizontal component of movement in the direction normal to the hill axis.

Three distinct causes, whose effects cannot be easily separated, could explain such phenomena. The first one is the quick

erosion process that is deepening the two valleys that border the Eastern and Western sides of the hill explaining the vertical and horizontal East–West component of movements. The second cause is the seismicity of the area. Earthquakes cause some opening of fractures in the platform. The strongest events can also trigger excess pore pressures in the clay shales underlying the slab, leading to some post-seismic subsidence that adds to effects of erosion. The global effect of such phenomena should then be a continuous deformation of the hill due to erosion enhanced by transient accelerations induced by earthquakes. As shown by available data, both processes have a long evolution due to the low permeability of the clay shale deposit and its high depth. The third cause is the occurrence of shallow and slow landslides favoured by erosion, which involve the boundaries of the slab causing outward movements. As a result, the platform is narrowing. A fourth cause, which unfortunately cannot be checked by satellite images, might be a northward component of movement due to the evolution of a deep and ancient landslide.

The described deformation process is very slow and complex. Recognized by some Authors as a spread or as a deep-seated gravitational slope deformation, due to its features and complexity, it has here been classified as a soil slope deformation (Hungri et al. 2014). It is probably active since thousands of years and will probably be active over further hundreds of years.

Acknowledgements

This research has been supported by MIUR PON R&I 2014-2020 Program (project MITIGO, ARS01_00964).

Declarations

Conflict of interest The authors declare no competing interests.

Open Access This article is licensed under a Creative Commons Attribution 4.0 International License, which permits use, sharing, adaptation, distribution and reproduction in any medium or format, as long as you give appropriate credit to the original author(s) and the source, provide a link to the Creative Commons licence, and indicate if changes were made. The images or other third party material in this article are included in the article's Creative Commons licence, unless indicated otherwise in a credit line to the material. If material is not included in the article's Creative Commons licence and your intended use is not permitted by statutory regulation or exceeds the permitted use, you will need to obtain permission directly from the copyright holder. To view a copy of this licence, visit <http://creativecommons.org/licenses/by/4.0/>.

References

- Alfano GB (1931) Il terremoto irpino del 1930. Osservatorio di Pompei.
- Bonardi G, D'Argenio B, Perrone V (1988) Carta geologica dell'Appennino meridionale alla scala 1:250.000. Mem Soc Geol It 41:1341
- Boschi E, Ferrari G, Gasperini P, Guidoboni E, Smeriglio G, Valensise G (1995) Catalogo dei forti terremoti in Italia dal 461 a.c. al 1980. ING-SGA.
- Costantini M, Ferretti A, Minati F, Falco S, Trillo F, Colombo D, Novali F, Malvarosa F, Mammone C, Vecchioli F, Rucci A, Fumagalli A, Allievi J, Ciminelli MG, Costabile S (2017) Analysis of surface deformations over the whole Italian territory by interferometric processing of ERS, Envisat and COSMOSkyMed radar data. Remote Sens Environ 202:250–275
- Crescenti U, Dramis F, Gentili B, Praturlon A (1984) The Bisaccia landslide: a case of deep-seated gravitational movement reactivated by earthquake. Actes du colloque "Mouvement de terrain." Caen, Document BRGM 83:15–21
- D'Argenio B, Pescatore T, Scandone P (1973) Schema geologico dell'Appennino meridionale (Campania e Lucania). Proc. Conf. Moderne vedute sulla geologia dell'Appennino, Acc. Naz. dei Lincei. Quaderni 183:49–72
- De Luca C, Zinno I, Manunta M, Lanari R, Casu F (2017) Large areas surface deformation analysis through a cloud computing P-SBAS approach for massive processing of DInSAR time series. Remote Sensing of the Environment 202:3–17
- Di Maio C, Fornaro G, Gioia D, Reale D, Schiattarella M, Vassallo R (2018) In situ and satellite long-term monitoring of the Latronico landslide, Italy: displacement evolution, damage to buildings, and effectiveness of remedial works. Eng Geol 245:218–235
- Di Marino F (2011) Evoluzione ed interpretazione dei fenomeni deformativi dell'abitato di Bisaccia. Unpublished Mr Thesis, Seconda Università di Napoli
- Di Martire D, Novellino A, Ramondini M, Calcaterra D (2016) A differential synthetic aperture radar interferometry of a deep seated gravitational slope deformation occurring at Bisaccia (Italy). Sci Total Environ 550:556–573
- Di Nocera S, Fenelli GB, Iaccarino G, Pellegrino A, Pescatore TS, Picarelli L (1995) An example on the geotechnical implications of geological history. Proc XI ECSMFE, Copenhagen 8:39–48
- Di Traglia F, De Luca C, Manzo M, Nolesini T, Casagli N, Lanari R, Casu F (2021) Joint exploitation of space-borne and ground-based multi-temporal InSAR measurements for volcano monitoring: the Stromboli volcano case study. Remote Sens Environ 260: 112441
- Fenelli GB, Picarelli L (1990) The pore pressure field built up in a rapidly eroded soil mass. Can Geotech J 27(3):387–392
- Fenelli GB, Picarelli L, Silvestri F (1992) Deformation process of a hill shaken by the Irpinia earthquake in 1980. Slope stability in seismic areas, Proc. French-Italian conf. 12–14 May, Faccioli, A. Pecker eds., Bordighera, 47–62. OuestÉditions
- Hungri O, Leroueil S, Picarelli L (2014) The Varnes classification of landslide types, an update. Landslides 11(2):167–194
- Koppula SD, Morgenstern NR (1984) Deficient pore pressures in an eroding soil mass. Can Geotech J 21:277–288
- Lampitiello S, Olivares L, Silvestri F (2001) Numerical simulation of seismic and post-seismic response of Bisaccia Hill. Lesson learned on recent strong earthquakes, Proc. TC4 Satellite Conference, 25–25 August, Istanbul
- Matheson DS, Thomson S (1973) Geological implications of valley rebound. Can J Earth Sci 10(6):961–978
- Oddone E (1931) Il terremoto dell'Irpinia del 23 luglio 1930 nell'Irpinia. L'Universo
- Ogniben L (1969) Schema introduttivo alla geologia del confine Calabro-lucano. Mem Soc Geol It 8:453–763
- Olivares L (1997) Caratterizzazione dell'argilla di Bisaccia in condizioni monotone, cicliche e dinamiche e riflessi sul comportamento del Colle a seguito del terremoto del 1980. PhD Thesis, Università di Napoli Federico II
- Olivares L, Picarelli L (1999) Discussion of the paper "A laboratory study of the strength of four stiff clays" by J.B. Burland, S. Rampello, V.N. Georgiannou & G. Calabresi. Géotechnique, 39, 2: 276–279
- Olivares L, Silvestri F (2001) A laboratory and numerical investigation on a post-seismic induced settlement in Southern Italy. Recent advances in geotechnical earthquake engineering and soil dynamics; Proc Fourth Int Conf, San Diego, California, 26–31 March 2001. Rotterdam: Balkema
- Picarelli L (2000) Mechanisms and rates of slope movements in fine grained soils. Proc Int Conf on Geotechnical and Geological Engineering GeoEng 2000, Melbourne, 1: 1618–1670.
- Picarelli L, Olivares L, Di Maio C, Silvestri F, Di Nocera S, Urciuoli G (2002) Structure, properties and mechanical behaviour of the highly plastic intensely fissured Bisaccia clay shale. In: Tan TS, Phoon KK, Hight, Leroueil S (eds) Proc. Int. Workshop on "Characterisation and Engineering

- Properties of Natural Soils", Singapore, vol 2. Balkema, Rotterdam, pp 947–982
- Picarelli L, Urciuoli G (1993) Effetti dell'erosione in argilliti di alta plasticità. Rivista Italiana Di Geotecnica 17:29–47
- Silvestri F (1997) Post-cyclic behaviour of stiff clays and likely effects on slope deformations. Discussion session IV (Slope stability and protection). Proc Int Symp on "Hard Soils and Soft Rocks", Athens, 3
- Urciuoli G (1992) Rigonfiamento di un'argilla di alta plasticità e modellazione de fenomeni erosivi del colle di Bisaccia. PhD. Thesis, Università di Napoli Federico II
- Varnes DJ (1978) Slope movement types and processes. In: Schuster RL, Krizek RJ (eds) Landslides, Analysis and Control, Special Report 176: Transportation Research Board. National Academy of Sciences, Washington, DC., pp 11–33
- Vassallo R, De Rosa J, Di Maio C, Reale D, Verde S, Fornaro G (2021) In situ and satellite long-term monitoring of two earthflows of the Italian southern Apennines and of the structures built on them. Italian Geotech J 55(4):77–95

L. Picarelli (✉)

Regional Models and Geo-Hydrological Impacts, Centro Euro-Mediterraneo sui Cambiamenti Climatici, CMCC, Lecce, Italy
Email: luciano.picarelli@unicampania.it

A. Santo · G. Di Crescenzo · G. Urciuoli · F. Silvestri

Università di Napoli Federico II, Naples, Italy

R. Vassallo

Università della Basilicata, Potenza, Italy

L. Olivares

Università della Campania, Naples, Italy

L. Picarelli

Università della Campania "Luigi Vanvitelli", Aversa, Italy
Email: luciano.picarelli@unicampania.it